

Multi-Target Localization of Breathing Humans

ChangKyeong Kim*, Joon-Yong Lee*, Taechong Cho†, Dongbok Ki*, Bong Ho Cho*, and Jihoon Yoon‡

*Dept. of Information & Technology, Handong University, Pohang 791-708, Korea

Email: paul3000@hgu.edu, joonlee@handong.edu, bokmanki@hanmail.net, crissmond@gmail.com

†Dept. of Nanobio Materials and Electronics, Gwangju Institute of Science and Technology

Oryong, Bukgu, Gwangju 500-712, Korea, Email: taechong@gist.ac.kr

‡Hyundai Mobis, Beon-gil, Mabuk, Giheung, Yongin, 446-912, Korea, Email: yauldk@naver.com

Abstract—In this paper, a technique for detecting the locations of one or more persons, as well as their breath patterns, using an ultra-wideband radar sensor network, is proposed. Technical problems that occur in the estimation process, such as false detection due to indirect reflection and ambiguity problem, are introduced. Maximum-likelihood estimation is suggested as the solution to these problems and tested on 10 sets of radar measurements.

I. INTRODUCTION

Ultra-wideband (UWB) signals have been proposed as the most suitable solution for applications performing accurate distance estimation because of their high resolution. Recently, considerable attention has been paid to the area of the detection of biological signals, such as those of a breathing pattern or heart rate, by detecting slight movement of a human body. Using the UWB radar, a breathing pattern of one or more persons can be detected along with distance and/or location information, and many studies on this technology have been conducted [1]–[13]. Additionally, there have been studies presenting experimental results on breathing pattern detection in an environment where a wall blocked the space between a person and the UWB radar [14]–[20]. To achieve this objective, the techniques of correlation detection, static background removal, and frequency analysis of breathing patterns have been used.

This study aims to detect a breathing pattern of one or more persons who breathe at a fixed position and their locations in a two-dimensional space. There are several technical difficulties in implementing the process. First, it is not easy to remove indirectly reflected signals reflected from static background along with a target person (this phenomenon is illustrated in section II greater in detail). These signals might be falsely detected as another target. In this paper, a technique for removing these multiple reflection signals involving the human body that screens them based on distance information and breathing pattern information of the detected potential targets is proposed. Second, when more than one person's locations are estimated based on the measured distance information by radar, ambiguity can arise. We used a maximum likelihood estimation technique to solve this problem.

This paper is organized as follows: section II introduces sets of radar measurements and its results. A process to detect distance and breathing frequencies of potential targets from the measured data is also shown in section II. In Section III, a

process for estimating the number and locations of breathing targets from the detected information is explained. Finally, test results of the estimation technique are presented in section IV.

II. RADAR MEASUREMENTS

UWB radar measurements were carried out using the Pulson P400 monostatic radar module manufactured by Time Domain, Inc. Each radar has two omni-directional dipole antennas attached so as to transmit and receive UWB pulses. The three radars were arranged in known locations and fixed on a foam pad to be placed at a height of about 0.7 m, which is near the average height of the chest a sitting adult. In addition, one to three people were positioned around the radars so that the breathing pattern and location of each person would be estimated. The location of each person was also determined in advance to evaluate the accuracy of the estimation. The relative location of each radar and person was measured using a laser distance measuring device. Ten sets of measurements were taken: five sets with one target, four sets with two targets, and one set with three targets.

The signal received at the i th radar can be expressed as $r^{(i)}(\tau; t)$, where the superscript (i) indicates the index for the radar, τ denotes the propagation delay of a reflected waveform and contains the distance information of a target, and t denotes the measurement time. When measuring received signals, each radar adopts an average for the transmission of 4096 pulses, thereby increasing the signal-to-noise ratio of the received signal. When the person to be detected takes a breath, a portion of body parts such as the chest and/or abdomen also moves according to a breathing pattern. This can change the structure of a multipath channel between the transmitting and receiving antennas of the radar, and as a result, the receiving signal also changes. Accordingly, by setting a receiving signal at a specific time as a reference signal, the difference between the measured signal and the reference signal is measured so that changes in signal components can be observed by removing static background signals. Let's denote the difference signal at a random moment t by $x^{(i)}(\tau; t)$.

For the timing detection of multipath signal components, matched filtering is performed. If the correlator template waveform is denoted by $s(\tau)$, correlation function $R_{xs, \text{BP}}^{(i)}(\Delta\tau; t)$ is obtained. Here, subscript "BP" indicates that the signal has been bandpass filtered. Our analysis used a Butterworth filter in the frequency band of 0.1Hz to 1.2Hz which corresponds

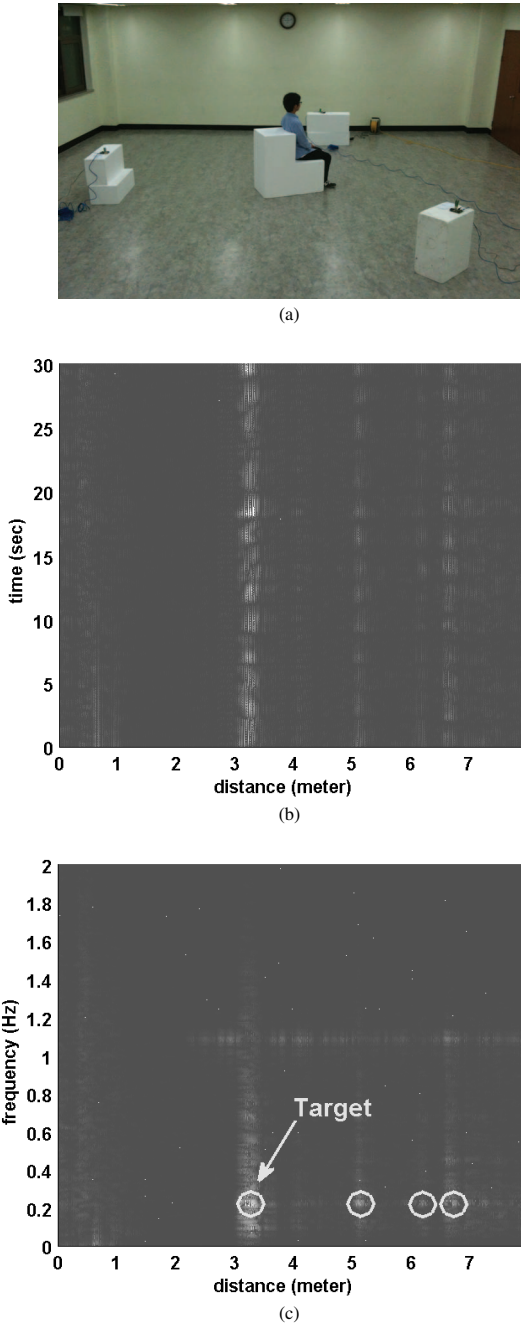


Fig. 1: (a) Experimental setup for one-person measurement. Plots of (b) $|R_{xs,BP}^{(3)}(r; t)|$ and (c) $|S_{xs,BP}^{(3)}(r; \lambda)|$.

to a general human breathing frequency band. In addition, by taking the Fourier transform of $R_{xs,BP}^{(i)}(\Delta\tau; t)$ with respect to variable t , spectral density $S_{xs}^{(i)}(\Delta\tau; \lambda)$ is obtained.

Figure 1 shows the measurement results in which one person breathes. Figure 1-(b) shows the plot of $|R_{xs,BP}^{(3)}(r; t)|$, where parameter r is the value that converts $\Delta\tau$ into distance. A periodic signal is observed at 3.2 m, which is the distance between the radar and the person. Additionally, a similar movement is detected at 5.1 m, 6.2 m, and 6.6 m, which was caused by the

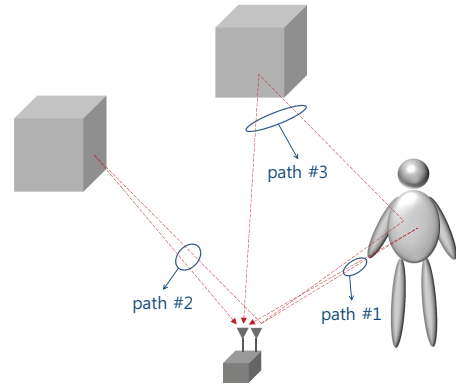


Fig. 2: Different kinds of reflections.

multiple reflection that includes the target and other objects on its reflection path. This phenomenon is also conspicuously observed in the frequency domain. Figure 1-(c) shows the plot of $|S_{xs,BP}^{(3)}(r; \lambda)|$. The breathing frequency and distance of the potential targets are determined by the following procedure. First, values of distance r where $\int_{-\infty}^{\infty} |S_{xs,BP}^{(i)}(r; \lambda)|^2 d\lambda$ has local peaks in the region where it exceeds the specific threshold are determined. Then, assuming that a value of the distance obtained here is denoted by r_j , find the values of frequency λ where $|S_{xs,BP}^{(i)}(r_j; \lambda)|$ has peaks in the region satisfying $|S_{xs,BP}^{(i)}(r_j; \lambda)| > \theta \cdot \max_{\lambda} |S_{xs,BP}^{(i)}(r_j; \lambda)|$. The points indicated by the circle in Figure 1-(c) represent the distance and frequency information detected using the method described in the above. Among the several points detected, only one contains the information on the actual target distance and breathing frequency, whereas the other points are all erroneously detected. Figure 2 illustrates this phenomenon. In the figure, path #1 is the direct path reflected by a human body, path #2 receives static background signals, and path #3 contains indirect reflections from a human body and background objects together. When the reference signal is subtracted from the received signal, the indirectly reflected signal received via path #3 cannot be removed, whereas the static background signal can be removed. Because of this, a system might falsely detect another target other than the actual target.

Figures 3 shows the test environment in which two people are located, and the measurement results that were obtained at radar 2. The two people breathe at 0.21 Hz and 0.42 Hz, respectively, and the multiple signal components at three different ranges are observed. Interestingly, multiple frequency components are detected at 3.3 m. This is indeed the detection of the harmonic components due to the regular movements of the human body as a result of breathing.

The values detected through the above process at the i th

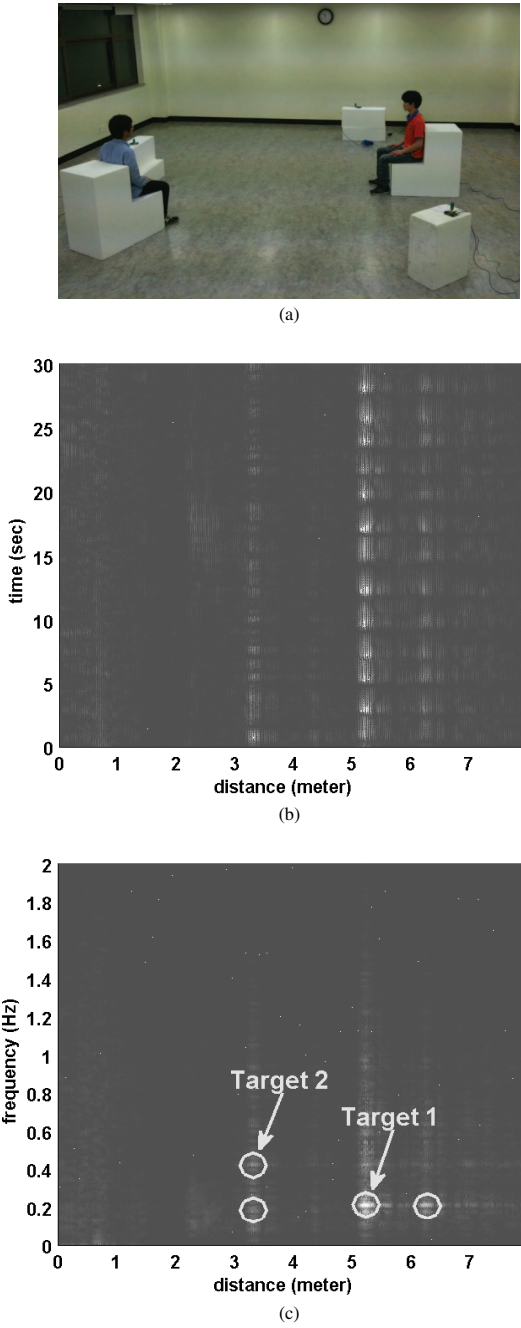


Fig. 3: (a) Experimental setup for two-person measurement. Plots of (b) $|R_{xs,BP}^{(2)}(r; t)|$ and (c) $|S_{xs,BP}^{(2)}(r; \lambda)|$.

radar can form a matrix

$$\mathcal{R}^{(i)} = \begin{bmatrix} (r_1^{(i)}, \lambda_1^{(i)}) \\ (r_2^{(i)}, \lambda_2^{(i)}) \\ \vdots \\ (r_{k_i}^{(i)}, \lambda_{k_i}^{(i)}) \end{bmatrix}, \quad (1)$$

where each row vector in the matrix indicate a detected point and it is assumed to satisfy $r_1^{(i)} \leq r_2^{(i)} \leq \dots \leq r_{k_i}^{(i)}$, $\forall i$. The

number of observation vectors is denoted by k_i . As already mentioned, matrix $\mathcal{R}^{(i)}$ can contain signal components received by indirect as well as direct reflections from the human body. In order to distinguish these signal components, an initial screening process is performed by analyzing the characteristics of the signal frequency. The rationale is as follows: human body movement due to breathing is significantly slower than the propagation delay of a signal, so it is highly probable that the movements of the directly and indirectly reflected signals from the human body are synchronized. For example, if $(r_j^{(i)}, \lambda_j^{(i)})$ and $(r_l^{(i)}, \lambda_l^{(i)})$ are vectors detected from the movement of the same person, and $r_j^{(i)} < r_l^{(i)}$, we can assume that $\lambda_j^{(i)} \simeq \lambda_l^{(i)}$. Furthermore, because these two points are where $|S_{xs,BP}^{(i)}(r; \lambda)|$ has local peaks, it can be assumed that both $S_{xs,BP}^{(i)}(\Delta\tau_j; \lambda_j)$ and $S_{xs,BP}^{(i)}(\Delta\tau_l; \lambda_l)$ have the same phase or phase difference of as large as π . Therefore, we can assume that two vectors that satisfy the following conditions are due to the movement of the same person and thereby remove $(r_l^{(i)}, \lambda_l^{(i)})$:

- 1) $|\lambda_j^{(i)} - \lambda_l^{(i)}| < \theta_\lambda$,
- 2) $|\angle S_{xs,BP}^{(i)}(r_j; \lambda_j) \pm \angle S_{xs,BP}^{(i)}(r_l; \lambda_l)| < \theta_p$,

where θ_λ and θ_p are thresholds, respectively. When more than two observations that satisfy the above conditions exist, a vector detected at the closest distance is chosen, and the others are removed by an assumption that they were detected because of indirect reflections. Now, a new matrix $\tilde{\mathcal{R}}^{(i)}$ is obtained by the result,

$$\tilde{\mathcal{R}}^{(i)} = \begin{bmatrix} (\tilde{r}_1^{(i)}, \tilde{\lambda}_1^{(i)}) \\ (\tilde{r}_2^{(i)}, \tilde{\lambda}_2^{(i)}) \\ \vdots \\ (\tilde{r}_{\tilde{k}_i}^{(i)}, \tilde{\lambda}_{\tilde{k}_i}^{(i)}) \end{bmatrix}, \quad (2)$$

where \tilde{k}_i is the number of remaining vectors left after removing observations due to indirect reflections. For example, in the experiment shown in Figure 1, $k_3 = 4$ and $\tilde{k}_3 = 2$ are obtained when $\theta_p = \frac{\pi}{25}$ and $\theta_\lambda = 0.004$, respectively. It is noted that the number of the remaining vectors is still greater than the actual number of targets. The next section presents methods to estimate the number, location, and breathing pattern of targets using the matrix $\tilde{\mathcal{R}}^{(i)}$ obtained from each radar.

III. MULTI-TARGET LOCATION

If the number of breathing objects that exist around a given radar is n , n satisfies

$$1 \leq n \leq N = \min_{1 \leq i \leq 3} \tilde{k}_i. \quad (3)$$

If the location of the j th target is φ_j , $1 \leq j \leq n$, and the two-dimensional spatial point in which the i th radar is located is $\underline{\alpha}^{(i)}$, the distance between the j th target and i th radar, namely

$d_j^{(i)}$, can be defined as

$$d_j^{(i)} = \left\| \underline{\alpha}^{(i)} - \underline{\varphi}_j \right\|. \quad (4)$$

Here, we try to estimate the locations of n targets, $\{\underline{\varphi}_1, \underline{\varphi}_2, \dots, \underline{\varphi}_n\}$, using observation matrices $\tilde{\mathcal{R}}^{(i)}$ s. In this process, various complex numbers of cases can occur. Firstly, there is the number of cases in which n vectors are selected from \tilde{k}_i observations obtained from the i th radar. If we let this number be Q_i , then

$$Q_i = \binom{\tilde{k}_i}{n}, \quad (5)$$

and the number of cases that select n observations from each $\tilde{\mathcal{R}}^{(i)}$ s becomes $\prod_{i=1}^3 Q_i$. Now we can make $(n!)^2$ different combinations, which is the number of cases that makes n groups comprising three vectors by selecting one vector from each $\tilde{\mathcal{R}}^{(i)}$. Therefore, when the number of potential targets is assumed to be n , the possible total number of combinations, M_n becomes

$$M_n = (n!)^2 \cdot \prod_{i=1}^3 \binom{\tilde{k}_i}{n}. \quad (6)$$

If this is expressed using a matrix, it can also be exhibited as

$$\mathcal{C}_{n,m} = \begin{bmatrix} \left(a_{1,n,m}^{(1)}, b_{1,n,m}^{(1)} \right), \dots, \left(a_{n,n,m}^{(1)}, b_{n,n,m}^{(1)} \right) \\ \left(a_{1,n,m}^{(2)}, b_{1,n,m}^{(2)} \right), \dots, \left(a_{n,n,m}^{(2)}, b_{n,n,m}^{(2)} \right) \\ \left(a_{1,n,m}^{(3)}, b_{1,n,m}^{(3)} \right), \dots, \left(a_{n,n,m}^{(3)}, b_{n,n,m}^{(3)} \right) \end{bmatrix}, \quad (7)$$

where the i th row is the permutation of n vectors selected from the matrix $\tilde{\mathcal{R}}^{(i)}$, while the first row is arranged such that $a_{1,n,m}^{(1)} \leq a_{2,n,m}^{(1)} \leq \dots \leq a_{n,n,m}^{(1)}$. Index m is the index that indicates one of M_n possible combinations and satisfies $1 \leq m \leq M_n$. Therefore, the total possible number of the matrix $\mathcal{C}_{n,m}$ becomes $\sum_{n=1}^N M_n$, which means the number of ambiguities.

Now, let us estimate the location of each target based on matrix $\mathcal{C}_{n,m}$. Define a vector $\hat{\underline{\varphi}}_{j,n,m}$ as the estimated location of the j th target. The estimated range between the i th radar and j th target, $\hat{d}_{j,n,m}^{(i)}$ is given by

$$\hat{d}_{j,n,m}^{(i)} = \left\| \underline{\alpha}^{(i)} - \hat{\underline{\varphi}}_{j,n,m} \right\|. \quad (8)$$

The error between the estimated and measured distances, $\delta_{j,n,m}^{(i)}$ can be defined as

$$\delta_{j,n,m}^{(i)} = a_{j,n,m}^{(i)} - \hat{d}_{j,n,m}^{(i)}, \quad (9)$$

where, $a_{j,n,m}^{(i)}$ is the measured distance between the i th radar and j th target designated by matrix $\mathcal{C}_{n,m}$. When the measurement errors of the distances are assumed to be independent, identically distributed (i.i.d.) random variables, each of which has $f_\delta(\delta)$ as its marginal density, the location of the j th target

can be estimated through maximum likelihood estimation as follows:

$$\hat{\underline{\varphi}}_{j,n,m} = \arg \max_{\underline{\varphi}} \prod_{i=1}^3 f_\delta \left(a_{j,n,m}^{(i)} - \left\| \underline{\alpha}^{(i)} - \underline{\varphi} \right\| \right). \quad (10)$$

If we further assume that

$$f_\delta(\delta) = \frac{1}{\sigma_\delta \sqrt{2\pi}} e^{-\delta^2/2\sigma_\delta^2}, \quad (11)$$

then least squares estimation can be applied to give

$$\hat{\underline{\varphi}}_{j,n,m} = \arg \min_{\underline{\varphi}} \sum_{i=1}^3 \left[a_{j,n,m}^{(i)} - \left\| \underline{\alpha}^{(i)} - \underline{\varphi} \right\| \right]^2. \quad (12)$$

The breathing frequency of each target can be estimated in a similar manner. When $\mathcal{C}_{n,m}$ is given, if the estimate of the breathing frequency of the j th target is assumed to be $\hat{\lambda}_{j,n,m}$, the error between this estimate and the breathing frequency measured in the i th radar becomes $\epsilon_{j,n,m}^{(i)} = b_{j,n,m}^{(i)} - \hat{\lambda}_{j,n,m}$. When the measurement errors of the breathing frequencies are assumed to be i.i.d. Gaussian random variables with means of 0 and variances of σ_ϵ^2 , $\hat{\lambda}_{j,n,m}$ can be obtained by using least squares estimation as follows:

$$\hat{\lambda}_{j,n,m} = \arg \min_{\lambda} \sum_{i=1}^3 \left(b_{j,n,m}^{(i)} - \lambda \right)^2. \quad (13)$$

Because the number of combinations is M_n , assuming the existence of n targets, the number of estimates that can be obtained of the location and breathing frequency of each target becomes M_n , respectively. Among the estimates, one estimate should be selected for each parameter, namely $\hat{\underline{\varphi}}_{j,n}$ and $\hat{\lambda}_{j,n}$. If M_n combinations are assumed to all be equiprobable, then $\hat{\underline{\varphi}}_{j,n} = \hat{\underline{\varphi}}_{j,n,\mu_n}$ and $\hat{\lambda}_{j,n} = \hat{\lambda}_{j,n,\mu_n}$, where

$$\mu_n = \arg \min_m \mathcal{L}(n, m). \quad (14)$$

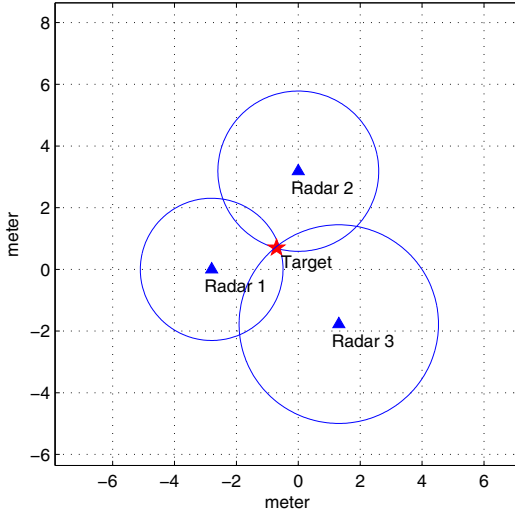
In the above equation, the cost function $\mathcal{L}(n, m)$ is defined as

$$\mathcal{L}(n, m) = \sum_{j=1}^n \sum_{i=1}^3 \left[\left(\frac{d_{j,n,m}^{(i)}}{\sigma_\delta} \right)^2 + \left(\frac{\epsilon_{j,n,m}^{(i)}}{\sigma_\epsilon} \right)^2 \right]. \quad (15)$$

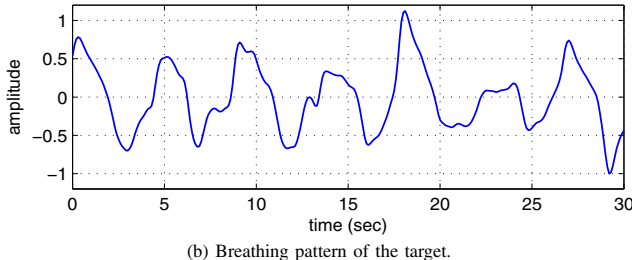
Finally, the number of targets, n should be determined. Finding the optimal value of n is a difficult task. When the value of n exceeds the number of actual targets, a large increase in the cost function $\mathcal{L}(n, \mu_n)$ can be predicted. In light of this, the present study obtained the estimate of n , namely ν , by calculating the rate of $\mathcal{L}(n, \mu_n)$ according to n and applying a threshold as follows:

$$\nu = \arg \max_n \left[\frac{1}{n} \mathcal{L}(n, \mu_n) < \theta_L \right], \quad (16)$$

where θ_L is the threshold value. Hence, the resulting estimates for the location and breathing frequency of the j th target can be obtained as $\hat{\underline{\varphi}}_j = \hat{\underline{\varphi}}_{j,\nu}$ and $\hat{\lambda}_j = \hat{\lambda}_{j,\nu}$, respectively.



(a) Estimated location the target.



(b) Breathing pattern of the target.

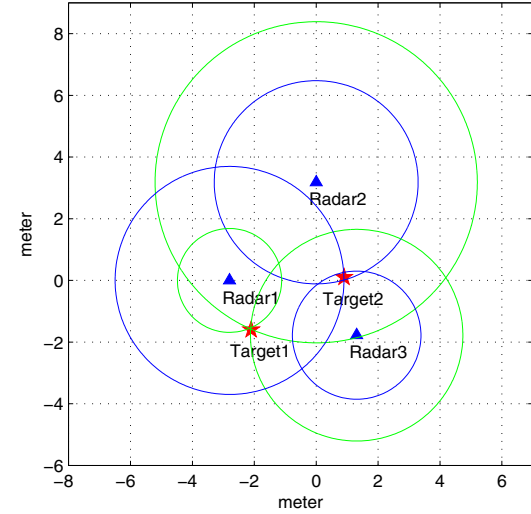
Fig. 4: The estimated location and resulting breathing pattern for one-person experiment shown in Figure 1 obtained with $\sigma_\delta^2 = 2.5 \times 10^{-3}$, $\sigma_\epsilon^2 = 2.5 \times 10^{-5}$, and $\theta_L = 20$.

IV. TEST RESULTS

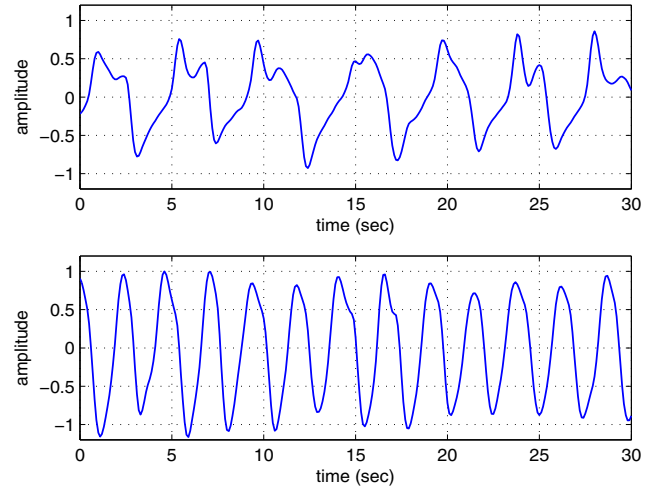
As mentioned in the previous section, there exist ambiguities in the process of estimating the location and breathing pattern of the targets. By applying the detection technique for the location and breathing pattern of the targets presented in Sections III, we can remove these ambiguities. Figure 4 and 5 show the results of removing the ambiguity that occurs during the estimation of the location and the resulting breathing pattern. Table I summarizes the test results for the 10 measurement sets. High accuracy of the estimation of the number and locations of the targets is achieved in spite of a large number of ambiguities.

V. CONCLUSIONS

The present study proposed a detection technique for the location and breathing pattern of an unknown number of people. The algorithm proposed in this study was applied to 10 data sets measured in an indoor office environment and exhibited a significantly high level of estimation accuracy. Among the contents suggested by the study, the process of detecting signal components that occur due to the motions resulting from breathing and, based on its outcome, detecting breathing patterns basically took a similar approach to that introduced in existing studies. However, this study has its



(a) Estimated locations of the targets.



(b) Breathing pattern of target 1 (upper) and target 2 (lower).

Fig. 5: The estimated locations and resulting breathing patterns for two-person experiment shown in Figure 3 obtained with $\sigma_\delta^2 = 2.5 \times 10^{-3}$, $\sigma_\epsilon^2 = 2.5 \times 10^{-5}$, and $\theta_L = 20$.

unique contribution in terms of using the technique that estimates the number, location, and breathing pattern of the targets after removing a number of ambiguities and prevents false detection caused by factors such as the harmonic components of the breathing frequencies and indirectly reflected signals received by successive reflections from the human body and the surrounding objects.

VI. ACKNOWLEDGEMENTS

This research was supported by the Basic Science Research Program through the National Research Foundation of Korea (NRF) funded by the Ministry of Education, Science and Technology (2010-0025422).

REFERENCES

- [1] M. Baboli, O. Boric-Lubecke, and V. Lubecke, "A new algorithm for detection of heart and respiration rate with UWB signals," in *34th Annual International Conference of the IEEE EMBS*, pp. 3947–3950, Aug. 2012.

TABLE I: Test results.

measurement number	number of targets	number of ambiguities	estimated number of targets	location error (m)			estimate of breathing frequency (Hz)		
				target 1	target 2	target 3	target 1	target 2	target 3
1	1	24	1	0.1393			0.23		
2		12	1	0.1397			0.21		
3		21	1	0.1709			0.20		
4		2	1	0.1239			0.26		
5		4	1	0.0634			0.30		
6	2	1,314	2	0.0831	0.1134		0.23	0.44	
7		17,208	2	0.2087	0.1583		0.41	0.17	
8		171	2	0.0350	0.2501		0.21	0.42	
9		24	2	0.0184	0.0221		0.24	0.24	
10	3	1,201,420	3	0.0572	0.3174	0.1334	0.26	0.48	0.18

- [2] Y. Chen, E. Gunawan, K. S. Low, Y. Kim, C. B. Soh, A. R. Leyman, and L. L. Thi, "Non-invasive respiration rate estimation using Ultra-Wideband Distributed Cognitive Radar system," in *Engineering in Medicine and Biology Society, 2006. EMBS '06. 28th Annual International Conference of the IEEE*, pp. 920–923, Sept. 2006.
- [3] W. Chunming and D. Guoliang, "The study of uwb radar life-detection for searching human subjects," in *2012 International Conference on Future Electrical Power and Energy System*, pp. 1028–1033, Feb. 2012.
- [4] K. Higashikaturagi, Y. Nakahata, I. Matsunami, and A. Kajiwara, "Non-invasive respiration monitoring sensor using UWB-IR," in *IEEE International Conference on Ultra-Wideband, 2008. ICUWB 2008.*, pp. 101–104, Sept. 2008.
- [5] Il'moreev, "UWB radar for patient monitoring," *Aerospace and Electronic Systems Magazine, IEEE*, vol. 23, pp. 11–18, Nov. 2008.
- [6] O. Kosch, F. Thiel, F. S. di Clemente, M. Hein, and F. Seifert, "Monitoring of human cardio-pulmonary activity by multi-channel UWB-radar," in *2011 IEEE-APS Topical Conference on Antennas and Propagation in Wireless Communications (APWC)*, pp. 382–385, Sept. 2011.
- [7] J. C. Y. Lai, Y. Xu, E. Gunawan, E. C.-P. Chua, A. Maskooki, Y. L. Guan, K.-S. Low, C. B. Soh, and C.-L. Poh, "Wireless sensing of human respiratory parameters by low-power Ultrawideband impulse radio radar," *IEEE Transaction on instrumentation and measurement*, vol. 60, pp. 928–923, Mar. 2011.

- [8] A. Lazaro, D. Girbau, and R. Villarino, "Analysis of vital signs monitoring using an ir-UWB radar," *Progress In Electromagnetics Research*, vol. 100, pp. 265–284, 2010.
- [9] M. Leib, W. Menzel, B. Schleicher, and H. Schumacher, "Vital signs monitoring with a UWB radar based on a correlation receiver," in *Proceedings of the Fourth European Conference on Antennas and Propagation (EuCAP), 2010*, pp. 1–5, April 2010.
- [10] K. Ota, Y. Ota, M. Otsu, and A. Kajiwara, "Elderly-care motion sensor using UWB-IR," in *Sensors Applications Symposium (SAS), 2011, IEEE*, pp. 159–162, Feb. 2011.
- [11] N. V. Rivera, S. Venkatesh, C. Anderson, and R. M. Buehrer, "Multi-target estimation of heart and respiration rates using Ultra wideband sensors," in *European Signal Processing Conference*, Sept. 2006.
- [12] J. Salmi, S. Sangodoyin, and A. F. Molisch, "High resolution parameter estimation for Ultra-Wideband MIMO radar," in *Record of the Forty Fourth Asilomar Conference on Signals, Systems and Computers (ASILOMAR), 2010 Conference*, pp. 2129–2133, Nov. 2010.
- [13] A. Sharafi, M. Baboli, M. Eshghi, and A. Ahmadian, "Respiration-rate estimation of a moving target using impulse-based ultra wideband radars," *Australas Phys Eng Sci Med*, Mar. 2012.
- [14] M. Y. W. Chia, S. Leong, C. Sim, and K. Chan, "Through-wall UWB radar operating within FCC's mask for sensing heart beat and breathing rate," in *European Radar Conference, 2005. EURAD*, pp. 267–270, Oct. 2005.
- [15] B. Levitas and J. Matuzas, "Uwb radar for breath detection," in *11th International Radar Symposium (IRS), 2010*, pp. 1–3, June 2010.
- [16] W. Li, X. Jing, Z. Li, and J. Wang, "A new algorithm for through wall human respiration monitoring using GPR," in *2012 14th International Conference on Ground Penetrating Radar*, pp. 947–952, June 2012.
- [17] J. Li, L. Liu, Z. Zeng, and F. Liu, "Simulation and signal processing of UWB radar for human detection in complex environment," in *14th International Conference on Ground Penetrating Radar (GPR), 2012*, pp. 1–3, June 2012.
- [18] J. Sachs, M. Aftanas, S. Crabbe, M. Drutarovsk, R. Klukas, D. Kocur, T. Nguyen, P. Peyerl, J. Rovnakova, and E. Zaikov, "Detection and tracking of moving or trapped people hidden by obstacles using ultra-wideband pseudo-noise radar," in *European Radar Conference, 2008. EuRAD 2008*, pp. 408–411, Oct. 2008.
- [19] S. Singh, Q. Liang, D. Chen, and L. Sheng, "Sense through wall human detection using UWB radar," *EURASIP Journal on Wireless Communications and Networking*, Jan. 2011.
- [20] E. Zaikov, "Uwb radar for detection and localization of trapped people," in *11th International Radar Symposium (IRS), 2010*, pp. 1–4, June 2010.